Supplementary File 1 for "What Launch Life Cycle Assessment Should Count for Starship-Scale Fleets: Ozone Health Damage Factors and a Failed Warming Potential"

Jiawei Jing

Makuhari Development Corporation, Chiba, Japan

Corresponding author: Jiawei Jing (jiawei.jing@mkhr.co.jp)

ORCID: https://orcid.org/0009-0000-8365-367X

Abbreviations: BC, black carbon; Cly, chlorine species; DU, Dobson unit; pEI, primary emission index; LH_2, liquid hydrogen; UDMH, unsymmetrical dimethylhydrazine; NMSC, non-melanoma skin cancer; COPD, chronic obstructive pulmonary disease; SCUP-h, Skin Cancer Utrecht–Philadelphia action spectrum, human; TOA, top of the atmosphere; SE, standard error; fixed-SST, fixed sea surface temperatures; IRF, instantaneous radiative forcing; GWP100, 100-yr global warming potential; AGWP100, absolute GWP100; AR6, Sixth Assessment Report; MAC, mass absorption cross section; EESC, equivalent effective stratospheric chlorine; SBUV, Solar Backscatter Ultraviolet.

Text S1. Emission Inventory

Primary emission indices (g/kg propellant; low, central, high) for BC are 20, 22, and 50 for RP-1; 4.69, 5, and 5 for methane at the low value and 20, 22, and 25 for methane treated as RP-1; 0 for LH_2; and 4, 16, and 25 for solid motors and UDMH. Primary Cly from solid motors is about 213 g/kg as Cl, and primary Al_2O_3 is 328 g/kg. Fuel NOx is 15.33 g NO_2/kg for UDMH and zero otherwise.

Afterburning follows Barker et al. (2024). With h in km, thermal NOx is 33 exp(−0.26 h) g NO/kg and $EI_{CO}(h) = \min[pEI_{CO}, 0.0025 \exp(0.067\ h)(pEI_{CO} + pEI_{CO}2)]$, with CO_2 from carbon balance. Total NOx is expressed as NO_2. Burn profiles use 1 km bins and a bin above 100 km. Effective indices are mass-weighted over the bins of a layer, with the index evaluated at the bin midpoint. CO_2 includes the bin above 100 km and afterburned CO. NOx at or above 15 km includes the bin above 100 km, which is nonzero only for UDMH.

Table 1 gives layered emissions per tonne of propellant, and Table S2 the resulting damage. Cly damage is paired with Cly mass in 15–50 km because the responses are stratospheric. Applied to the 2022 fleet below 80 km, this inventory matches Barker et al. (2024) within 6% for seven species and total propellant (Figure S1b).

The NOx response of Larson et al. (2017) is divided by the emissions of a 0–28 km air-breathing trajectory and applied here to mass at or above 15 km. If the response came only from stratospheric emissions, the factor per kilogram would be larger; NOx is about 2%–3% of UV damage for Falcon 9 with all-altitude mass and under 0.1% with mass at or above 15 km.

Text S2. Ozone-to-Health Chain

For disease d and latitude band b, added DALY are $B_d \times w_{d,b} \times RAF_{d,b} \times BAF_d \times \Delta O_{3,b} / TOC_b$, where B is the global burden for 2015 (WHO 2026) and TOC_b is the 1979–1981 SBUV column (NASA Goddard Space Flight Center n.d.). For skin cancers, $w_{d,b}$ is the share of global DALY in responding regions (Zhang et al. 2021, for 2019; melanoma 63%, squamous cell carcinoma 34%, basal cell carcinoma 80%) spread over bands by the regional map of Table S5, and NMSC burden is split between carcinoma types by DALY share. Responding regions are Western, Central, and Eastern Europe, Australasia, high-income North America, and Southern Latin America. By incidence these regions hold 96% of squamous cell carcinoma, but by DALY only 34%, because DALY per case outside these regions is 45 times that inside them, and it is the DALY share that scales damage.

The radiation amplification factor (RAF) for skin cancer is 1.15 (1.1–1.2), the SCUP-h value of UNEP (1998), with a melanoma lower end of 0.1 for a UVA-dominated action spectrum. The biological amplification factors (BAF) are those of Table 3 of Madronich et al. (2021): melanoma 0.54, the mean of the sex-specific values, with a range of 0.415–0.702 that we widen because the published errors are standard errors of the fit only; basal cell carcinoma 1.4 (0.95–1.85); squamous cell carcinoma 2.6 (1.85–3.35); zero for darker skin; and cataract 0.17 (0.08–0.26) for lighter skin and 0.24 (0.15–0.33) for others. Latitude-resolved cataract RAF ranges from about 1.10 near the equator to 1.29 at 60–70°N, with a ±27% action spectrum uncertainty. Cataract burden is spread by total population.

The unresolved difference between cataract routes is treated as a structural choice and is not sampled in the Monte Carlo. Cataract totals by route: WHO fraction 1,261; pig-lens spectrum (U.S. EPA 2010) 3,747; central 5,790; UNEP (1998) static estimate 44,543; prevalence route 95,300 DALY/(DU·yr), with crude incidence weighted by the 2010 age structure (102,000 with that of 2015). The central cataract chain applies a cortical cataract amplification to all cataract burden, which U.S. EPA (2010) notes may overstate the effect. Allocation by incidence share, with bands weighted by lighter-skinned population and a UV exponent, gives 20,067 DALY/(DU·yr) for the same base year. These routes move burden between latitudes and so change the BC shape factor: Table S6 gives their effect on BC, along with responding regions and the regional map.

CFC-11 check. Against Hayashi and Itsubo (2023), for 2015, melanoma and NMSC are higher by factors of 1.50 and 1.51, and cataract is lower at 0.34. The total hides two offsetting differences. Ozone loss per kilogram of CFC-11 is 0.0178 %·yr/Gg here, 0.0181 from the scenario estimate of WMO (2022), and 0.0052 from slopes (their Figure S2) and ΔEESC of Hayashi and Itsubo (2023). Their value implies about 60,000 DALY/(DU·yr), or 5.3 times ours on global-mean DU. With their ozone loss and the prevalence cataract route, this chain reaches 0.87 of their total, so the cataract route accounts for most of that gap. The melanoma term here is 1,900 DALY/(DU·yr), against 7,600 from the skin cancer term of Eastham et al. (2018).

The shape factor for a species is $\Sigma_b\, c_b\, \Delta O_{3,b} / (\Sigma_b\, c_b \times \Delta O_{3,\mathrm{global}})$, where c_b is the chain coefficient per DU in band b. It is computed from annual means at central parameters. In the interactive-ocean output it is 1.7–2.1, but the product of ozone change and shape factor agrees with the fixed-SST runs within 6%.

The co-benefit is -83×10^{-9} deaths per person-year per DU $\times$ 7.455×10^{9} persons $\times$ 19.05 DALY per death, using years of life lost per death above age 30 because Eastham et al. (2018) evaluate adults above 30, with meteorological variability of 0.93–1.30. Years lived with disability are excluded because the concentration–response function refers to mortality; COPD and asthma years lived with disability would raise the term by about 29%. Its triangular distribution has support of −27,000 to −802 DALY/(DU·yr). The lowermost-stratosphere case replaces the 83 with 260 + 0.5 × 39 deaths per 10^{9} person-years per DU: Eastham et al. (2018) give the net for that experiment without a skin cancer term, which we take as half of the 39 of their all-stratosphere experiment.

Text S3. Use of the Factors and Monte Carlo

Using the factors. Apply Equation 1 and Text S1 to the vehicle's burn profile to get mass by layer; Table 1 gives this for the LEAT trajectories only. Multiply by the UV damage of Table 2; the P5 and P95 of different species sum to an upper envelope, because they share one health chain. Report the total without BC, then the BC line, at 5 and 22 g/kg for methane engines. Report the co-benefit separately. Use the 100-yr CO_2 factor as primary and the 500-yr factor as a sensitivity (Fantke et al. 2026). Do not add these factors to ozone depletion potential-based or surface-release factors for the same emission. Table 2 applies to launch emissions and not to re-entry. Al_2O_3 is reported as mass only. Supplementary File 2 holds Tables 1 and 2 in machine-readable form (emissions_by_layer_per_tonne.csv, factors_launch_emissions.csv). The BC factor averages 10–100 Gg/yr; at 10 Gg/yr alone it is about 1.3 times the P50.

Worked example, one Starship launch at 5 g/kg: 3.8 t of BC in 15–70 km $\times$ 2.9×10^{-3} DALY/kg gives 11 DALY, against 2,457 t of CO_2 $\times$ 1.5×10^{-6} DALY/kg = 3.7 DALY over 100 yr.

Damage for a launch or fleet is $(m_{BC}\, L_{BC}\, S + m_{Cly}\, L_{Cly} + m_{NOx}\, L_{NOx}) \times \mathrm{UV}$, where L is ozone loss per kilogram, S is the BC shape factor by case (1.49, 1.59, and 1.53 at 10, 30, and 100 Gg/yr), and UV is damage per DU·yr at uniform DU. The three BC cases and the three Cly cases each carry equal weight. UV and the co-benefit are drawn from triangular distributions with the central value as mode and supports fitted to the chain's P5 and P95. The net of UV damage and co-benefit is negative with probability 0.27 for BC and 0.64 for uniform DU (Cly, NOx), on the central altitude shape and concentration–response function.

Ratios to CO_2 carry no uncertainty in the CO_2 factor, and non-combustion life cycle CO_2 is not included in the denominator. Payload capacities are 100 t for Starship (Space Exploration Technologies Corp. 2026) and 17.5 t for Falcon 9 (Ohs et al. 2025). The 145 launches a year are caps of 25, 44, and 76 at three sites (Department of the Air Force 2025; Federal Aviation Administration 2025, 2026).

Text S4. Public Model Output and the Warming Test

Maloney et al. (2022). We read the zonal-mean output for control, 10, 30, and 100 Gg/yr: column ozone, air temperature at the lowest model level, and BC. Column ozone is the sum over layers of O3 mixing ratio × dry pressure thickness / (g × molar mass of air), and global means use cosine-latitude weights. Table S3 compares the published table, latitude means without area weighting, and area-weighted means.

Seam in the interactive-ocean files. These runs are stored in two segments, joined at the start of 2034; the second carries the suffix "_rad_bc", whose meaning we could not establish. Total BC burden falls between December 2033 and January 2034 from 494 to 124 Gg at 100 Gg/yr, from 219 to 122 Gg at 30 Gg/yr, and from 148 to 120 Gg at 10 Gg/yr, near the control value, and returns to its former level by about 2038. The fixed-SST files show no such discontinuity. Excluding 2034–2038 changes ΔT to −0.03, −0.08, and −0.11 K from 0.00, −0.04, and −0.11 K. Over the excluded years ΔT is +0.28, +0.21, and −0.09 K. Five-year means over 2010–2033 have a standard deviation of 0.08 and 0.11 K at 10 and 30 Gg/yr, so the excluded mean is unusual at 10 Gg/yr, matched in size only by the −0.21 K of 2015–2019 at 30 Gg/yr, and may be related to the seam. Negative lag-1 correlations are treated as zero in the standard errors.

SOCOLv4. The public files of Revell and Sukhodolov (2024) hold monthly zonal means of total column ozone and air temperature for 2034–2059. Differences from the reference run reproduce the reported 60°S–60°N ozone changes of the all-species ambitious and conservative runs (0.95 and 0.55 DU against 0.95 and 0.56 DU). Ocean temperatures respond in these runs. The temperature field is missing where a level lies below the surface, so the means cover latitudes with complete data; 940 hPa covers most of the globe, and 902 hPa gives the same change within 0.01 K (Table S4).

Implied ΔT. A GWP100 multiplied by the CO_2 temperature integral (4.3×10^{-14} K·yr/kg over 100 yr) gives a temperature integral I. For sustained emission E this implies $\Delta T = E \times I \times R$, where R = 0.88 is the mean two-box response over years 10–50 relative to the 100-yr response (0.87 over years 10–36 for SOCOLv4). For a lifetime of about 3 yr the convolution changes this by under 2%. At 1.7 Gg/yr, the BC emission of the all-species conservative run, the implied warming is about 0.10 K and the run cannot separate it from zero. The IRF route implies 0.10 K at 10 Gg/yr, against an upper bound near 0.04 K; it rests on a steady-state scaling of the published forcing, so we do not treat that dose as a failure. The stratospherically adjusted forcing route uses a GWP100 of -1.7×10^5, from the steady-state value in Table S1 with the AR6 carbon-cycle term (-1.6×10^5 without it) and without an efficacy, and implies −0.065, −0.20, and −0.65 K at 10, 30, and 100 Gg/yr.

Forcing. The GWP100 of $1.60 \times 10^6 \times$ AGWP100(CO_2) of 8.9×10^{-14} W·yr/(m²·kg) gives 142 mW/m² per Gg/yr, which is the steady forcing per unit of sustained emission for any lifetime well under 100 yr. Divided by a lifetime of 4 yr and multiplied by Earth's area of 5.1×10^{14} m², it gives about 18 MW/kg; the excess over absorbable sunlight holds for lifetimes under about 5.5 yr, while the comparison in mW/m² per Gg/yr does not depend on lifetime. Sunlight absorbed in

a thin layer is the mass absorption cross section × 340 W/m^2 × (2 + 2α). A particle intercepts the direct beam at any solar zenith angle during the half of the time it is sunlit, and light reflected from below, with planetary albedo α ≈ 0.3, contributes 2α × 340 W/m^2. This gives 6.6 MW/kg at 7.5 m^2/g (Bond and Bergstrom 2006) and 13 MW/kg at 15 m^2/g, a lensing factor of 2.

Text S5. Conditions and Other Pathways

Model structure. BC burden in SOCOLv4 is about 30 Gg, a lifetime of about 7.2 yr against 3.2–3.7 yr in CESM2-WACCM6, and ozone loss per unit burden is 0.022 against 0.031–0.051 DU/Gg, both from runs with an interactive ocean. Combining the sensitivity of one model with the lifetime of the other gives 0.075–0.36 DU per Gg/yr, or ×0.42 to ×2.0 on the BC factor. GISS ModelE reports BC burdens of 92, 110, and 298 for control, 1,000, and 10,000 launches a year, printed partly in Tg; its stated whole-atmosphere lifetimes of 5.3, 6.4, and 17 days confirm Gg, a rocket BC lifetime of about 2.1–2.5 yr. Its 0.11 and 0.063 DU/Gg at the two doses with the SOCOLv4 lifetime give ×4.5 and ×2.5.

Absorption of UV-B by BC. For BC burden increment M, τ_{abs}(310 nm) = M × MAC(550 nm) × (550/310) / A with A = 5.1 × 10^{14} m^2, and the fractional surface loss is τ_{abs}/μ_0. Central values use MAC 7.5 m^2/g and μ_0 = 0.7, with extremes of 5.96 m^2/g and 0.8, and 11.25 m^2/g and 0.5. The ozone effect uses 0.39% per DU. Scattering and clouds are neglected. With the SOCOLv4 BC burden the offset is about 44%.

BC above 70 km. Equation 1 leaves all primary BC in place above about 42 km, so a long upper-stage burn adds mass outside the layer. At 5 g/kg one Starship launch puts 9.2 t of BC above 70 km. Where that BC goes, in particular above 100 km, is unknown. CESM2-WACCM6 omits second-stage emissions, and GISS ModelE has a model top near 65 km.

Surface-ozone co-benefit. The lowermost-stratosphere experiment of Eastham et al. (2018) gives −39,702 DALY/(DU·yr) against −11,790 in their all-stratosphere experiment. Population-weighted surface ozone change in the BC runs is 1.5 times its global mean, but the factor of Eastham et al. (2018) already carries its own population weighting, so we do not scale it. With the shape factor on UV damage only, the concentration–response function of Turner et al. (2016) gives a BC net ozone damage of −17,000 DALY/(DU·yr), and that of the Global Burden of Disease for chronic obstructive pulmonary disease gives about +10,000.

BC climate term. Read through the GLAM factor, the simulated cooling at 100 Gg/yr would be a benefit 5–24 times BC UV damage, and at lower doses the range spans both signs. We do not recommend this translation, for the reasons in Section 4.1.

Emissions below 15 km. A Starship launch emits 30 t of NOx, nearly all below 15 km. With fine-particulate damage factors of 5–12 × 10^{-4} DALY per kg $PM_{2.5}$-equivalent (Sugiyama et al. 2025) and 0.1–0.2 kg $PM_{2.5}$-equivalent per kg NOx (0.11 in Huijbregts et al. 2016), this gives 1.5–7.1 DALY. About 69% of this NOx is released below 2 km, so surface-release factors apply to most of it, at global-average exposure and not that of the launch site.

Re-entry. NOx uses the UV damage per kilogram re-entering at a yield of 0.27 kg NO_2/kg: 0.031 –0.21 DALY per 100 t with Larson et al. (2017) and 7.8 DALY with the transient response of Vliex et al. (2026). For Al_2O_3, Maloney et al. (2025) report regional maxima of about −3 to −5.5 DU in the Northern Hemisphere and up to about +9 DU in the Southern Hemisphere. These are not global means, so we give no DALY for them.

Stratospheric water vapor. In GISS ModelE stratospheric water vapor rises by about 7% and 50% with BC at 1,000 and 10,000 launches a year, against 1% and 2% from direct injection (Tsigaridis et al. 2024). The two add roughly linearly, and the BC-driven part already sits inside the simulated BC response, so reporting the injected mass understates this pathway at large doses.

Choices fixed after inspecting results. Area weighting and the exclusion of 2034–2038; the 2015 base year, regional DALY allocation, and shape factor; the Cly mass layer; keeping out of the Monte Carlo a residual cataract factor derived from the comparison with Hayashi and Itsubo (2023), because it would calibrate the chain to one published total (medians about 16% lower than with it); and resting each factor on one source, with GISS ModelE as a check.

Table S1. *Atmospheric Responses Used, per Unit Sustained Emission*

Species	Quantity	Central	Range	Unit	Source
BC	ΔO_3, CESM2-WACCM6, 10 Gg/yr	−0.221	−0.315 to −0.127	DU per Gg/yr	Maloney et al. (2022), public output, area-weighted
BC	ΔO_3, CESM2-WACCM6, 30 Gg/yr	−0.182	−0.198 to −0.167	DU per Gg/yr	Maloney et al. (2022), public output, area-weighted
BC	ΔO_3, CESM2-WACCM6, 100 Gg/yr	−0.129	−0.137 to −0.121	DU per Gg/yr	Maloney et al. (2022), public output, area-weighted
BC	ΔO_3, GISS ModelE, 1,000 launches/yr (check)	−0.238	−0.298 to −0.179	DU per Gg/yr	Tsigaridis et al. (2024)
BC	ΔO_3, GISS ModelE, 10,000 launches/yr (check)	−0.155	−0.161 to −0.149	DU per Gg/yr	Tsigaridis et al. (2024)
BC	ΔO_3, SOCOLv4, 4.25 Gg/yr (check)	−0.156	−0.37 to 0.059	DU per Gg/yr	Revell et al. (2025), public output, area-weighted
BC	ΔT, interactive ocean, CESM2-WACCM6, 10 Gg/yr	−0.00349	−0.0107 to 0.00369	K per Gg/yr	Maloney et al. (2022), public output, area-weighted
BC	ΔT, interactive ocean, CESM2-WACCM6, 30 Gg/yr	−0.00261	−0.00537 to 0.000153	K per Gg/yr	Maloney et al. (2022), public output, area-weighted
BC	ΔT, interactive ocean, CESM2-WACCM6, 100 Gg/yr	−0.0011	−0.00181 to −0.00038	K per Gg/yr	Maloney et al. (2022), public output, area-weighted
BC	ΔT, interactive ocean, SOCOLv4, 4.25 Gg/yr (check)	−0.00012 7	−0.0224 to 0.0222	K per Gg/yr	Revell et al. (2025), public output, area-weighted
BC	IRF, scaled to steady state	20.2	17.6 to 25.1	mW/m² per Gg/yr	Barker et al. (2026)
BC	Stratospherically adjusted forcing, scaled to steady state	−14.4	−17.8 to −12.5	mW/m² per Gg/yr	Barker et al. (2026)
Cly	ΔO_3, Rocket10, 60°S–60°N annual	−0.0222	−0.0267 to −0.0178	DU per Gg/yr	Li et al. (2026)
Cly	ΔO_3, Rocket52, 60°S–60°N annual	−0.0231	−0.0247 to	DU per Gg/yr	Li et al. (2026)

Species	Quantity	Central	Range	Unit	Source
Cly	ΔO_3, Rocket120, 60°S–60°N annual	−0.0218	−0.0216 −0.0232 to −0.0205	DU per Gg/yr	Li et al. (2026)
NOx	ΔO_3, ascent emissions	−0.00357	−0.00393 to −0.0021	DU per Gg/yr	Larson et al. (2017), simulation 3

Note. Each value is the steady-state anomaly divided by the emission rate. Ranges encode reported or computed interannual variability (area-weighted cases: ±2 standard errors with lag-1 autocorrelation) or rounding of the published values (GISS ModelE: 2 and 13 DU at 8.4 and 84 Gg/yr, used as point values; weighting not stated in the source). The NOx case is divided by the emissions of a 0–28 km trajectory. The cases of Maloney et al. (2022) share one control run.

Table S2. *Damage per Tonne of Propellant*

Propellant	BC pEI (g/kg)	UV damage, case range (DALY/t)	CO_2, 100 yr (DALY/t)
RP-1	22	0.00982 to 0.0164	0.00148
Methane	5	0.0018 to 0.00301	0.000805
Methane	22	0.0079 to 0.0132	0.000805
Liquid hydrogen	0	5.59×10^{-7}	0
Solid motors	16	0.032 to 0.04	0.000696
UDMH	16	0.00789 to 0.0129	0.000339

Note. Masses are in Table 1.

Table S3. *Maloney et al. (2022): Published Table 1, Latitude Means of the Public Output Without Area Weighting, and Area-Weighted Means*

Run	Quantity	Published	Unweighted (± 2 SE)	Area-weighted (± 2 SE, autocorrelation)
Control	Column ozone (DU)	280	281.5	274.7
Control	All-sky TOA net flux (W/m^2)	−29	−28.6	+1.5
Control	Clear-sky TOA net flux (W/m^2)	−6.0	−6.0	+27.8
10 Gg/yr	Column ozone (DU)	−3.5	−3.56 ± 1.34	−2.21 ± 0.936
10 Gg/yr	ΔT (K)	−0.007	−0.008 ± 0.0853	0.005 ± 0.0909
10 Gg/yr	ΔT excluding 2034–2038 (K)			−0.0349 ± 0.0717
10 Gg/yr	All-sky TOA flux (W/m^2)	0.076	0.0756 ± 0.118	−0.005 ± 0.14
10 Gg/yr	Clear-sky TOA flux (W/m^2)	0.002	0.002 ± 0.112	−0.0616 ± 0.107
30 Gg/yr	Column ozone (DU)	−9.05	−9.13 ± 1.09	−5.47 ± 0.469
30 Gg/yr	ΔT (K)	−0.083	−0.0824 ± 0.0815	−0.0417 ± 0.101
30 Gg/yr	ΔT excluding 2034–2038 (K)			−0.0782 ± 0.0828
30 Gg/yr	All-sky TOA flux (W/m^2)	0.15	0.146 ± 0.114	0.007 ± 0.133
30 Gg/yr	Clear-sky TOA flux (W/m^2)	−0.056	−0.0558 ± 0.102	−0.132 ± 0.0711
100 Gg/yr	Column ozone (DU)	−20	−20.4 ± 1.26	−12.9 ± 0.768
100 Gg/yr	ΔT (K)	−0.19	−0.19 ± 0.0803	−0.107 ± 0.0606
100 Gg/yr	ΔT excluding 2034–2038 (K)			−0.11 ± 0.0717
100 Gg/yr	All-sky TOA flux (W/m^2)	0.47	0.47 ± 0.113	0.119 ± 0.129
100 Gg/yr	Clear-sky TOA flux (W/m^2)	−0.13	−0.128 ± 0.109	−0.306 ± 0.0862

Note. Rows at 10, 30, and 100 Gg/yr are changes from control. Means over 2010–2049. Ozone and fluxes are fixed-SST runs; temperature is the lowest model level in interactive-ocean runs, against surface temperature in the published table. The published ± values are close to the unweighted 2 standard errors without autocorrelation, including 0.085 K at 10 Gg/yr, printed as 0.85.

Table S4. *SOCOLv4 Runs of Revell et al. (2025) Minus the Reference Run, Public Output, 2034 –2059 (± 2 SE With Autocorrelation)*

Run	Global column ozone (DU)	60°S–60°N column ozone (DU)	T at about 940 hPa (K)	T at about 902 hPa (K)
BC only, 4.25 Gg/yr	−0.66 ± 0.91	−0.53 ± 0.69	0.00 ± 0.09	0.00 ± 0.09
Gas-phase species only	−0.74 ± 1.50	−0.56 ± 1.43	−0.03 ± 0.13	−0.03 ± 0.13
Al_2O_3 only	+0.74 ± 1.26	+0.32 ± 1.14	−0.05 ± 0.12	−0.06 ± 0.12
All species, ambitious	−1.38 ± 1.02	−0.95 ± 0.85	0.00 ± 0.09	0.00 ± 0.08
All species, conservative	−0.82 ± 1.43	−0.55 ± 1.19	+0.04 ± 0.10	+0.04 ± 0.10

Note. Area-weighted annual means. The 940 hPa mean covers 93% of the globe and the 902 hPa mean 97%, the latitudes with complete data. The BC-only run at about 970 hPa is +0.05 ± 0.11 K over 73% of the globe, a masking effect because the excluded latitudes are colder at 940 hPa. All rows share one reference run. At 4.25 Gg/yr the GWP route implies 0.26 K and the IRF route 0.04 K over the same window. Global BC-only ozone by half of the run: −0.33 and −1.00 DU. BC burden in the all-species ambitious run, 2050–2059: 30 Gg, from the public particle number density for a radius of 120 nm and density of 1.8 g/cm³, or a lifetime of 7.2 yr; the public files hold no burden for the BC-only run.

Table S5. *Approximate Population Shares Used to Place Global Burden of Disease Regions in Latitude Bands*

Region	Bands
Western Europe (responds)	60–70°N 5%; 50–60°N 45%; 40–50°N 40%; 30–40°N 10%
Central Europe (responds)	50–60°N 30%; 40–50°N 70%
Eastern Europe (responds)	60–70°N 10%; 50–60°N 75%; 40–50°N 15%
North America, high income (responds)	50–60°N 10%; 40–50°N 33%; 30–40°N 45%; 20–30°N 12%
Australasia (responds)	20–30°S 20%; 30–40°S 70%; 40–50°S 10%
Southern Latin America (responds)	20–30°S 5%; 30–40°S 80%; 40–50°S 15%
Asia Pacific, high income	40–50°N 7%; 30–40°N 90%; 0–10°N 3%
Central Asia	40–50°N 50%; 30–40°N 50%
East Asia	40–50°N 15%; 30–40°N 50%; 20–30°N 35%
South Asia	30–40°N 10%; 20–30°N 60%; 10–20°N 25%; 0–10°N 5%
Southeast Asia	20–30°N 10%; 10–20°N 35%; 0–10°N 25%; 0–10°S 30%
Caribbean	20–30°N 35%; 10–20°N 65%
Andean Latin America	0–10°S 55%; 10–20°S 45%
Central Latin America	20–30°N 55%; 10–20°N 25%; 0–10°N 20%
Tropical Latin America	0–10°S 25%; 10–20°S 35%; 20–30°S 40%
North Africa and Middle East	30–40°N 45%; 20–30°N 45%; 10–20°N 10%
Oceania	10–20°N 10%; 0–10°S 70%; 10–20°S 20%
Central Sub-Saharan Africa	0–10°N 30%; 0–10°S 50%; 10–20°S 20%
Eastern Sub-Saharan Africa	10–20°N 15%; 0–10°N 30%; 0–10°S 35%; 10–20°S 20%

Region	Bands
Southern Sub-Saharan Africa	10–20°S 5%; 20–30°S 70%; 30–40°S 25%
Western Sub-Saharan Africa	10–20°N 45%; 0–10°N 55%

Note. Assigned by hand from the locations of major population centers and used only for the band weights of the skin cancer burden; the map of the responding regions drives the result. Regions not marked responding enter only the all-regions alternative.

Table S6. *Sensitivity of the UV Health Chain to Responding Regions and the Regional Map*

Chain variant	Uniform DU (DALY/(DU·yr))	BC shape factor	BC, relative	Cly, relative
Lighter-skinned regions (central)	11,248	1.54	1.00	1.00
East Asia also responds	14,761	1.52	1.30	1.31
East Asia and high-income Asia Pacific also respond	15,056	1.52	1.32	1.34
All regions respond	20,506	1.26	1.49	1.82
Responding regions one band north	11,027	1.84	1.17	0.98
Responding regions one band south	11,649	1.29	0.87	1.04
WHO cataract fraction	6,720	1.86	0.72	0.60
Prevalence cataract route	100,760	0.91	5.27	8.96
Burden allocated by incidence	20,067	0.87	1.01	1.78

Table S7. *UV Damage, Net Ozone Damage, and Combustion CO_2 per Launch and per Year of Launches (DALY)*

Vehicle or fleet	UV damage, P50 (P5–P95)	Net ozone damage, P50 (P5–P95)	CO_2, 100 yr; 500 yr	UV ÷ CO_2, 100 yr; 500 yr
Falcon 9	5.8 (3.8 to 9.5)	1.3 (−2.2 to 4.8)	0.67; 3.0	8.6; 1.9
Starship, BC 5 g/kg	11 (7.0 to 18)	2.4 (−4.1 to 9.0)	3.7; 17	2.9; 0.65
Starship, BC 22 g/kg	48 (31 to 78)	10 (−18 to 40)	3.7; 17	13; 2.8
2022 fleet	1,020 (690 to 1,610)	180 (−470 to 810)	75; 330	14; 3.0
2029 projection	2,510 (1,700 to 3,990)	450 (−1,140 to 2,020)	190; 840	13; 3.0
Ariane 62†	9.1 to 11	0.57 to 1.1	0.20; 0.88	46–57; 10–13
Starship, 145 launches a year, BC 5 g/kg†	1,760 to 2,940	550 to 880	790; 3,510	2.2–3.7; 0.50–0.84
Starship, 145 launches a year, BC 22 g/kg†	7,740 to 12,900	2,440 to 3,890	790; 3,510	9.8–16; 2.2–3.7

Note. Fleet rows are damage committed per year of launches. †Case range in place of the distribution. The net ranges exclude the altitude shape of the co-benefit and the concentration–response function (Text S5). Starship uses 4,658 t of propellant; the 145-launch rows use 6,750 t.

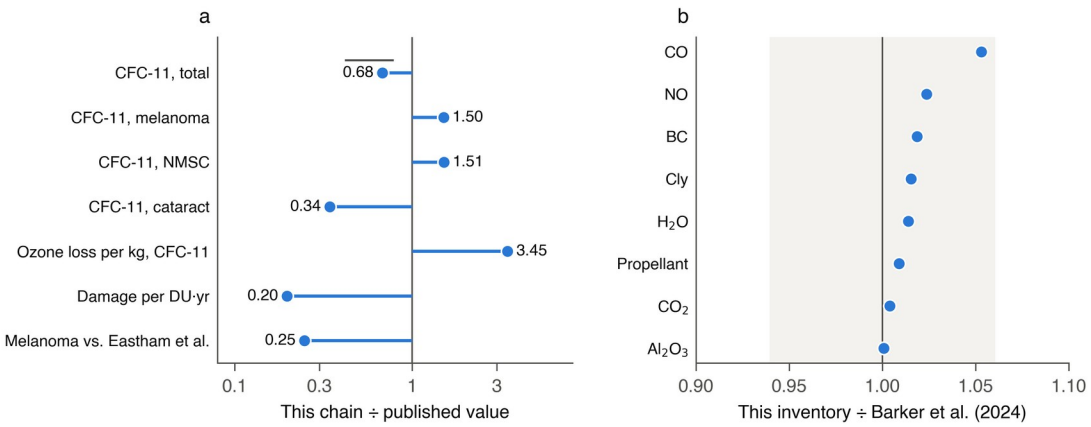


Figure S1. Benchmarks. (a) This chain against Hayashi and Itsubo (2023) for CFC-11, for the total with its Monte Carlo range and by disease, then ozone loss per kilogram and damage per DU·yr, and the melanoma term against Eastham et al. (2018). (b) Inventory check against Barker et al. (2024) for seven species and total propellant, 2022 fleet below 80 km. NMSC, non-melanoma skin cancer.

References

Barker CR, Marais EA, McDowell JC (2024) Global 3D rocket launch and re-entry air pollutant and CO_2 emissions at the onset of the megaconstellation era. Scientific Data 11:1079. https://doi.org/10.1038/s41597-024-03910-z

Barker CR, Marais EA, Tan EYP, Eastham SD, Diskin GS, DiGangi JP, Choi Y, Rollins AW, Waxman E, Bui TP, Gatebe CK, Dean-Day J, Poudyal R (2026) Radiative Forcing and Ozone Depletion of a Decade of Satellite Megaconstellation Missions. Earth's Future 14:e2025EF007229. https://doi.org/10.1029/2025ef007229

Bond TC, Bergstrom RW (2006) Light Absorption by Carbonaceous Particles: An Investigative Review. Aerosol Science and Technology 40:27-67. https://doi.org/10.1080/02786820500421521

Department of the Air Force (2025) Notice of record of decision for the environmental impact statement for SpaceX Starship-Super Heavy at Cape Canaveral Space Force Station, Florida. Federal Register. https://federalregister.gov/d/2025-23314

Eastham SD, Keith DW, Barrett SRH (2018) Mortality tradeoff between air quality and skin cancer from changes in stratospheric ozone. Environmental Research Letters 13:034035. https://doi.org/10.1088/1748-9326/aaad2e

Fantke P, Boulay AM, Cardinaals R, Debarre L, Huang L, Islam K, Kijko G, Levasseur A, Li D, Li S, Lloyd S, Margni M, Motoshita M, Namovich J, Oberschelp C, Paulillo A, Pfister S, Rupcic L, Scherer L et al (2026) A Global Consensus Life Cycle Impact Assessment Method (GLAM):

impacts on human health. The International Journal of Life Cycle Assessment 31:171. https://doi.org/10.1007/s11367-026-02742-w

Federal Aviation Administration (2025) Final tiered environmental assessment for SpaceX Starship/Super Heavy vehicle increased cadence at the SpaceX Boca Chica launch site in Cameron County, Texas. https://www.faa.gov/media/94346

Federal Aviation Administration (2026) Environmental impact statement for the SpaceX Starship-Super Heavy launch vehicle at Launch Complex 39A at the Kennedy Space Center, Merritt Island, Florida.

Hayashi K, Itsubo N (2023) Damage factors of stratospheric ozone depletion on human health impact with the addition of nitrous oxide as the largest contributor in the 2000s. The International Journal of Life Cycle Assessment 28:990-1002. https://doi.org/10.1007/s11367-023-02174-w

Huijbregts MAJ, Steinmann ZJN, Elshout PMF, Stam G, Verones F, Vieira MDM, Hollander A, Zijp M, van Zelm R (2016) ReCiPe 2016 v1.1: A harmonized life cycle impact assessment method at midpoint and endpoint level. Report I: Characterization (RIVM Report 2016-0104a). National Institute for Public Health and the Environment. https://www.rivm.nl/sites/default/files/2018-11/Report%20ReCiPe_Update_20171002_0.pdf

Larson EJL, Portmann RW, Rosenlof KH, Fahey DW, Daniel JS, Ross MN (2017) Global atmospheric response to emissions from a proposed reusable space launch system. Earth's Future 5:37-48. https://doi.org/10.1002/2016ef000399

Li Y, Feng W, Plane JMC, Wang T, Chipperfield MP (2026) The impact of rocket-emitted chlorine on stratospheric ozone. Atmospheric Chemistry and Physics 26:3621-3635. https://doi.org/10.5194/acp-26-3621-2026

Madronich S, Lee-Taylor JM, Wagner M, Kyle J, Hu Z, Landolfi R (2021) Estimation of Skin and Ocular Damage Avoided in the United States through Implementation of the Montreal Protocol on Substances that Deplete the Ozone Layer. ACS Earth and Space Chemistry 5:1876-1888. https://doi.org/10.1021/acsearthspacechem.1c00183

Maloney CM, Portmann RW, Ross MN, Rosenlof KH (2022) The Climate and Ozone Impacts of Black Carbon Emissions From Global Rocket Launches. Journal of Geophysical Research: Atmospheres 127:e2021JD036373. https://doi.org/10.1029/2021jd036373

Maloney CM, Portmann RW, Ross MN, Rosenlof KH (2025) Investigating the potential atmospheric accumulation and radiative impact of the coming increase in satellite reentry frequency. Journal of Geophysical Research: Atmospheres 130:e2024JD042442. https://doi.org/10.1029/2024JD042442

NASA Goddard Space Flight Center (n.d.) SBUV Merged Ozone Data Set (MOD), version 8.7. https://acd-ext.gsfc.nasa.gov/Data_services/merged/

Ohs R, Stock GF, Schmidt A, Fraire JA, Hermanns H (2025) Dirty bits in low-Earth orbit: The carbon footprint of launching computers. ACM SIGEnergy Energy Informatics Review 5:26-33. https://doi.org/10.1145/3757892.3757896

Revell L, Sukhodolov T (2024) Simulation data for 'Near-future rocket launches could slow ozone recovery'. Zenodo. https://doi.org/10.5281/zenodo.14183405

Revell LE, Bannister MT, Brown TFM, Sukhodolov T, Vattioni S, Dykema J, Frame DJ, Cater J, Chiodo G, Rozanov E (2025) Near-future rocket launches could slow ozone recovery. npj Climate and Atmospheric Science 8:212. https://doi.org/10.1038/s41612-025-01098-6

Space Exploration Technologies Corp (2026) Form S-1 registration statement. U.S. Securities and Exchange Commission. https://www.sec.gov/Archives/edgar/data/0001181412/000162828026036936/spaceexplorationtechnologi.htm

Sugiyama G, Onoda A, Nii S, Furuta C, Nakamura K, Itsubo N (2025) Integrating environmental and nutritional health impacts using disability-adjusted life years: Study using the Ajinomoto Group Nutrient Profiling System toward healthy and sustainable Japanese dishes. Sustainability 17:7977. https://doi.org/10.3390/su17177977

Tsigaridis K, Field R, Bauer SE, Ross MN, Maloney C, Schmidt GA, Rosenlof KH (2024) Composition and Climate Impacts of increasing launches to Low Earth Orbit. AIAA SCITECH 2024 Forum. https://doi.org/10.2514/6.2024-2168

Turner MC, Jerrett M, Pope CA, Krewski D, Gapstur SM, Diver WR, Beckerman BS, Marshall JD, Su J, Crouse DL, Burnett RT (2016) Long-Term Ozone Exposure and Mortality in a Large Prospective Study. American Journal of Respiratory and Critical Care Medicine 193:1134-1142. https://doi.org/10.1164/rccm.201508-1633oc

U.S. EPA (2010) Protecting the ozone layer protects eyesight: A report on cataract incidence in the United States using the Atmospheric and Health Effects Framework model. U.S. Environmental Protection Agency.

UNEP (1998) Environmental effects of ozone depletion: 1998 assessment. United Nations Environment Programme.

Vliex YSW, van 't Hoff JA, Dedoussi IC (2026) The Role of Propellant Type, Re-Entry, and Plume Reactions in the Atmospheric Impacts of Spaceflight. Earth's Future 14:e2025EF007795. https://doi.org/10.1029/2025ef007795

WHO (2026) Global health estimates 2023: DALYs, YLLs, YLDs, and deaths by cause, age and sex. World Health Organization. https://www.who.int/data/global-health-estimates

WMO (2022) Scientific assessment of ozone depletion: 2022 (GAW Report No. 278). World Meteorological Organization. https://csl.noaa.gov/assessments/ozone/2022/

Zhang W, Zeng W, Jiang A, He Z, Shen X, Dong X, Feng J, Lu H (2021) Global, regional and national incidence, mortality and disability-adjusted life-years of skin cancers and trend analysis from 1990 to 2019: An analysis of the Global Burden of Disease Study 2019. Cancer Medicine 10:4905-4922. https://doi.org/10.1002/cam4.4046